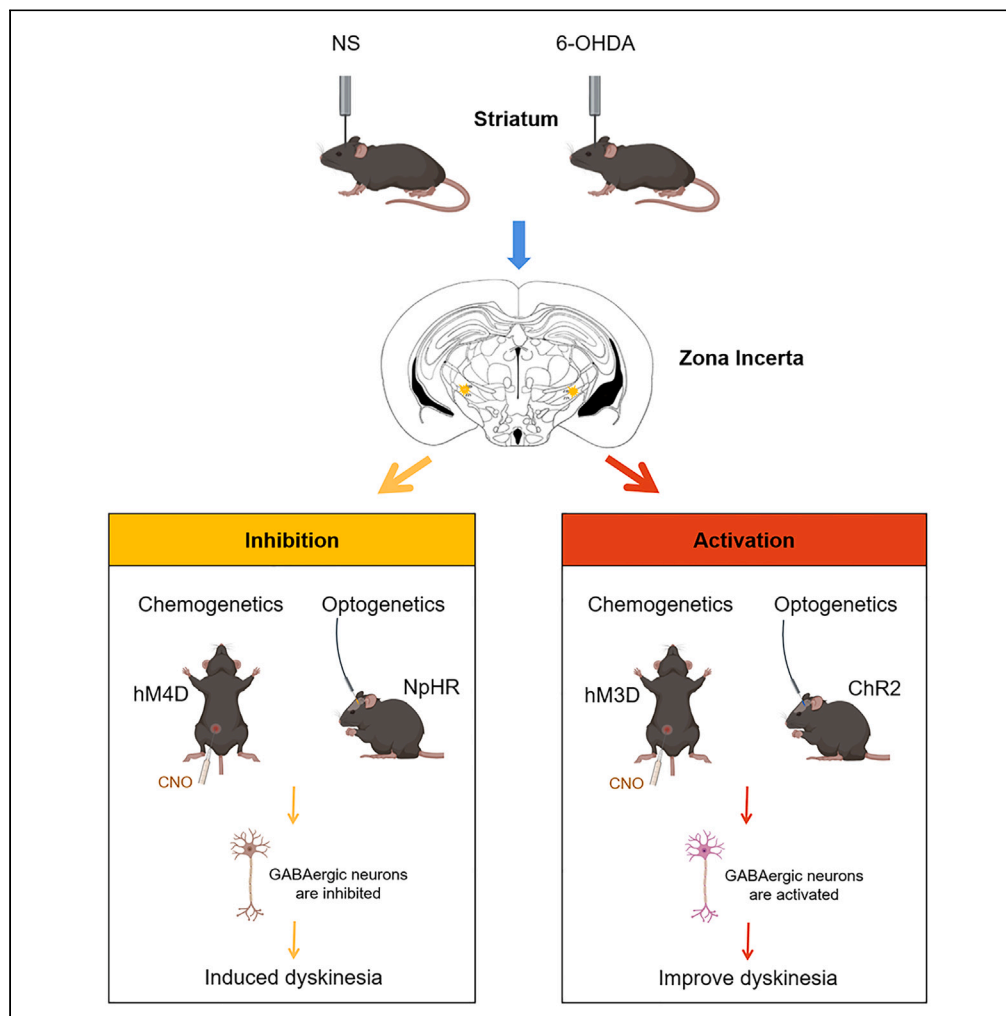


Article

Chemogenetic and optogenetic stimulation of zona incerta GABAergic neurons ameliorates motor impairment in Parkinson's disease



Fenghua Chen,
Junliang Qian,
Zhongkai Cao,
Ang Li, Juntao Cui,
Limin Shi, Junxia
Xie

liminshi@qdu.edu.cn (L.S.)
jxiexie@public.qd.sd.cn (J.X.)

Highlights

Zona incerta (ZI)
GABAergic neurons
impact parkinsonian
motor dysfunction

The number of GABA-
positive neurons in the ZI
was decreased in
6-OHDA-treated mice

Chemogenetic/
optogenetic activation of
ZI GABAergic neurons
improves PD mice
locomotion

Chemogenetic repeated
activation increases
striatal dopamine content

Chen et al., iScience 26,
107149
July 21, 2023 © 2023 The
Author(s).
[https://doi.org/10.1016/
j.isci.2023.107149](https://doi.org/10.1016/j.isci.2023.107149)

Article

Chemogenetic and optogenetic stimulation of zona incerta GABAergic neurons ameliorates motor impairment in Parkinson's disease

Fenghua Chen,^{1,2,3} Junliang Qian,^{2,3} Zhongkai Cao,^{1,2} Ang Li,^{1,2} Juntao Cui,^{1,2} Limin Shi,^{1,2,4,*} and Junxia Xie^{1,2,*}

SUMMARY

Parkinson's disease (PD) is characterized by the degeneration of dopaminergic neurons in the substantia nigra and leads to progressive motor dysfunction. While studies have focused on the basal ganglia network, recent evidence suggests neuronal systems outside the basal ganglia are also related to PD pathogenesis. The zona incerta (ZI) is a predominantly inhibitory subthalamic region for global behavioral modulation. This study investigates the role of GABAergic neurons in the ZI in a mouse model of 6-hydroxydopamine (6-OHDA)-induced PD. First, we found a decrease in GABA-positive neurons in the ZI, and then the mice used chemogenetic/optogenetic stimulation to activate or inhibit GABAergic neurons. The motor performance of PD mice was significantly improved by chemogenetic/optogenetic activation of GABAergic neurons, and repeated chemogenetic activation of ZI GABAergic neurons increased the dopamine content in the striatum. Our work identifies the role of ZI GABAergic neurons in regulating motor behaviors in 6-OHDA-lesioned PD model mice.

INTRODUCTION

Parkinson's disease (PD) is one of the most common neurodegenerative disorders, second to Alzheimer's disease.¹ Dopaminergic neuron loss in the substantia nigra pars compacta (SNc), which causes striatal dopamine (DA) deficiency, and intracellular α -synuclein aggregates are the neuropathological hallmarks of PD. Patients typically present with motor symptoms and signs, including bradykinesia, muscular rigidity, rest tremor, gait disturbance, and postural instability.² Levodopa is the most common first-line therapy; however, prolonged use often causes severe side effects marked by involuntary motor activity.³ Therefore, current research is directed toward identifying novel strategies for more effective treatment of this disorder. Currently, deep brain stimulation (DBS) is the most efficient symptomatic treatment.^{4,5}

Growing clinical studies have indicated that the zona incerta (ZI) may be a complementary target to the subthalamic nucleus (STN) in treating PD by DBS.⁶ The ZI is an inhibitory subthalamic region with extensive connections throughout the brain.^{7–9} Due to its multiple interconnections with the cerebral cortex, thalamus, brainstem, basal ganglia, spinal cord, and cerebellum, the ZI has been implicated in visceral activity, arousal, posture, locomotion, fear, anxiety, feeding, and the alleviation of PD.^{8,10–15} In earlier studies, high-frequency stimulation of the ZI was found to result in greater improvement in contralateral motor scores in PD patients than stimulation of the STN.¹⁶ A recent clinical report demonstrated that dual targeting of the STN and ZI is feasible and may provide additional benefits beyond conventional DBS of the STN alone in some PD patients. Bilateral ZI DBS alleviates motor symptoms, especially tremor, and improves activities of daily living and quality of life in PD patients.¹⁷ Moreover, ZI DBS has no negative impact on swallowing ability, body mass index, or cognitive function.^{18,19} Stimulation of the ZI also reduces experimentally induced thermal pain in PD patients.²⁰ Nevertheless, the mechanisms underlying the effect of ZI in PD therapy are not clear. Since the ZI is a predominantly inhibitory GABAergic nucleus, it is necessary to explore how these neurons affect parkinsonian symptoms.

In recent years, novel chemogenetic and optogenetic tools to modulate neuronal activity have been developed and applied to study neurodegenerative diseases.^{21,22} Chemogenetic methods involve the activation of designer receptors (genetically modified muscarinic receptors) exclusively activated by designer drugs (DREADDs) (clozapine-N-oxide, CNO). Optogenetics refers to a technique in which neural activity is

¹Department of Physiology, Shandong Provincial Key Laboratory of Pathogenesis and Prevention of Neurological Disorders, School of Basic Medicine, Qingdao University, Qingdao, China

²Institute of Brain Science and Disease, Qingdao University, Qingdao, China

³These authors contributed equally

⁴Lead contact

*Correspondence: liminshi@qdu.edu.cn (L.S.), jxiaxie@public.qd.sd.cn (J.X.)
<https://doi.org/10.1016/j.isci.2023.107149>



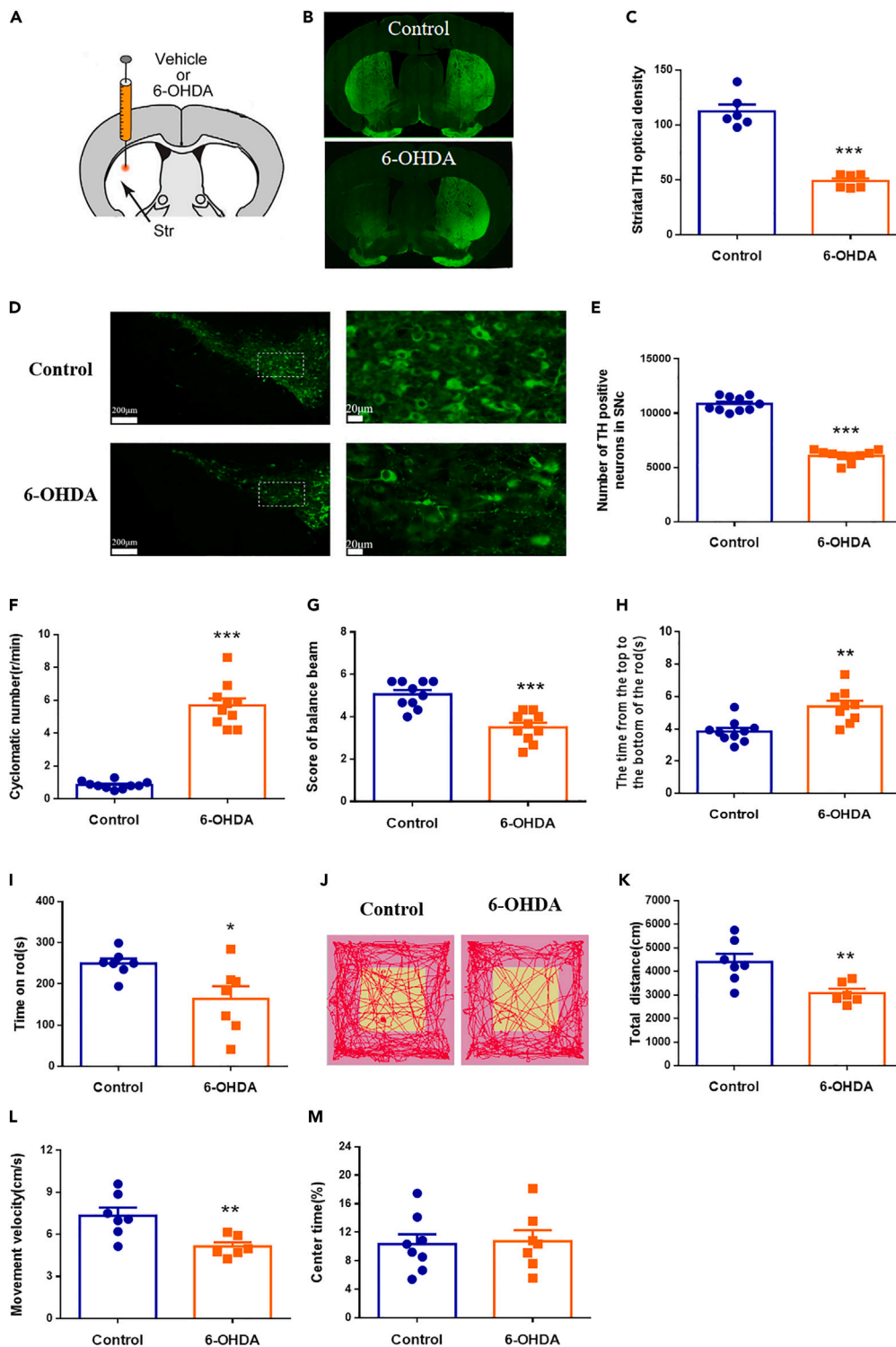


Figure 1. Unilateral striatal injection of 6-OHDA disrupts the nigrostriatal pathway

(A) Schematic illustration of the injection of 6-OHDA in the striatum.

(B and C) Sample images and statistical analysis showing that the density of TH⁺ fibers in the striatum was significantly reduced after 6-OHDA treatment.

(D and E) Sample images and statistical analysis showing that the number of TH⁺ neurons in the SN was significantly reduced after 6-OHDA treatment.

Figure 1. Continued

(F) 6-OHDA treatment increased the number of APO-induced rotations in the mice.

(G) 6-OHDA treatment decreased the score of passing the balance beam.

(H) The 6-OHDA-treated mice needed a longer time to climb from the top to the bottom of the rod in the pole test.

(I) The latency to fall from the accelerating rotating rod in 6-OHDA mice was decreased.

(J–M) Performance of 6-OHDA and control mice in the open-field test: track map (J), total movement distance (K), movement velocity (L), and center zone exploration time (M). Striatal injection of 6-OHDA induced bradykinesia in the open-field test. Each value is represented as means \pm SEM. All data were normally distributed, unpaired t-test was used, * $p < 0.05$, ** $p < 0.01$, *** $p < 0.001$, compared with Control, $n = 6–10$.

controlled by opsins, light-sensitive ion channels whose expression can be explicitly induced in neuronal populations of interest. Through chemogenetic and optogenetic activation and/or inhibition of GABAergic neurons, we aimed to determine whether GABAergic neurons in the ZI play a role in parkinsonian motor symptoms.

Currently, 6-hydroxydopamine (6-OHDA) is used to induce PD in mice. 6-OHDA is the most commonly used neurotoxin for eliminating dopaminergic neurons in the SNc and induces parkinsonian motor deficits.^{23–25} Using immunofluorescence staining, we showed that the number of GABA-positive neurons in the ZI was decreased in PD mice. Administration of etomidate or bicuculline into the ZI affected motor behavior. Finally, both chemogenetic and optogenetic activations of GABAergic neurons effectively reversed motor dysfunction.

RESULTS**Toxic effect of 6-OHDA on the nigrostriatal system and ZI**

To establish the PD model, we injected the neurotoxin 6-OHDA into the unilateral striatum (Figure 1A). The lesion extent was measured in three ways. First, we examined whether tyrosine hydroxylase (TH)-immunoreactive (TH⁺) terminals were present in the striatum. As shown in Figures 1B and 1C, at 14 days after 6-OHDA treatment, there were fewer TH⁺ terminals in the striatum in 6-OHDA-treated mice than in control mice, confirming that 6-OHDA injection had the intended effect. Second, we assessed whether there was a reduction in the number of TH⁺ neurons in the substantia nigra. Our quantitative analysis showed that unilateral 6-OHDA injection resulted in an average reduction in the number of TH⁺ neurons of 44.05% (Figures 1D and 1E). We also used several behavioral parameters to evaluate motor function: the number of rotations, the distance traveled and movement velocity in the open-field test, balance in the balance beam test, and coordination and integration in the pole test. The results showed that mice treated with 6-OHDA displayed marked impairment of all these behavioral parameters. At 14 days after 6-OHDA lesioning, APO administration (s.c.) induced rotation toward the uninjured side, with strong postural asymmetry. The average number of contralateral rotations per minute was 5.7. No circling behaviors were observed in the control groups (Figure 1F). 6-OHDA-treated mice had a lower average balance beam score than control mice (Figure 1G), took longer time to climb from the top of the pole to the bottom (Figure 1H), and exhibited an average reduction in the time spent on the rotating rod of 34.3% (Figure 1I). In the open-field test, the total distance traveled spontaneously was reduced in the 6-OHDA-treated group, and the average movement velocity was significantly reduced from 7.3 cm/s to 5.1 cm/s (Figures 1J–1L). We also examined anxiety-like phenotypes in the mice. No significant differences were found between the control and 6-OHDA groups in the time spent in the center of the arena (Figure 1M), indicating that anxiety-like behavior was unaffected. Together, these results indicate that unilateral striatal injection of 6-OHDA induces nigrostriatal system damage and parkinsonian motor symptoms.

GABA expression in the ZI is reduced after 6-OHDA lesioning

We next examined whether there were any changes in neurotransmitter expression in the ZI of 6-OHDA-lesioned mice. We focused on GABA expression because GABAergic neurons are abundant in number in the ZI. As shown in Figures 2A and 2B, the number of GABA-immunoreactive (GABA⁺) neurons was decreased. There was a 13% reduction in the number of GABA⁺ neurons in the 6-OHDA groups compared with the control groups. We also evaluated GABAergic subpopulations and the number of neurons expressing the calcium-binding protein parvalbumin (PV) in the ZI. As shown in Figures 2C and 2D, the number of PV⁺ neurons in the ZI was decreased by 34% in 6-OHDA-treated mice compared with NS-treated mice. Therefore, striatal 6-OHDA injection induces a major change in GABA expression within the ZI.

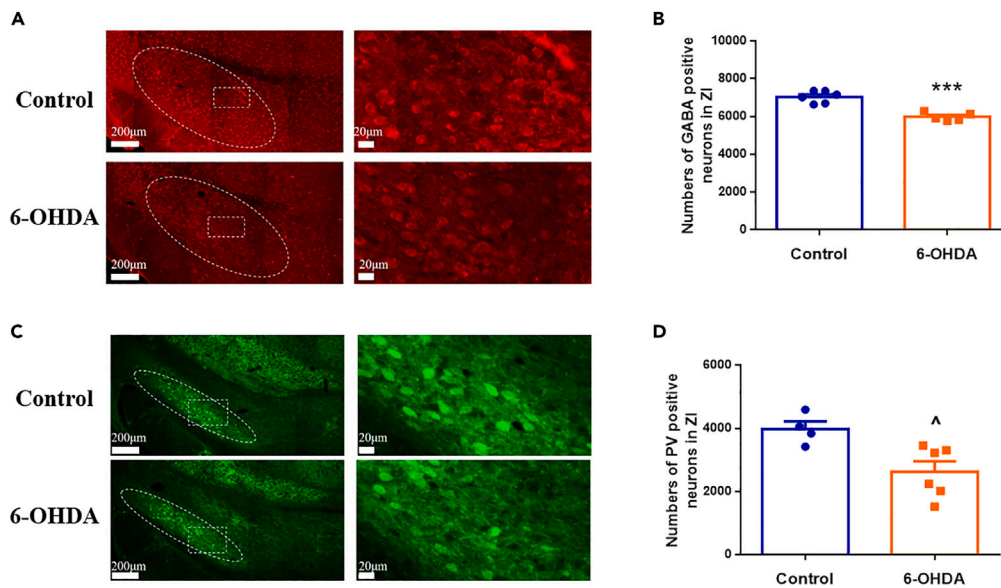


Figure 2. The neurochemical changes of GABAergic neurons in the ZI after 6-OHDA treatment

(A) Sample images showing GABA⁺ neurons in the ZI in the control and 6-OHDA treated groups. (B) Statistical analysis for A. The number of GABA⁺ neurons in the ZI was significantly reduced after 6-OHDA treatment. (C) Sample images showing PV⁺ neurons in the control and 6-OHDA treated groups. (D) Statistical analysis for C. The number of PV⁺ neurons in the ZI was significantly reduced after 6-OHDA treatment. Each value is represented as means \pm SEM. Data in (B) showed normal distribution, unpaired t-test was used, ***p < 0.001, compared with Control; Data in (D) showed nonnormal distribution, non-parametric test was used, \wedge p < 0.05, unpaired t-test, n = 6.

Pharmacological enhancement/suppression of the ZI GABAergic signaling affects motor behavior

To test the role of the ZI in motor behavior, we implanted a guide cannula into the ZI (Figure 3A). After recovery from implantation, we microinjected NS (1 μ L) or the GABA_A receptor agonist etomidate (5 μ g/ μ L, 1 μ L) into the mice and performed behavior tests. Infusion of etomidate into naive mice caused significant decreases in the total distance traveled and movement velocity in the open-field test but did not affect the central zone exploration time (Figures 3B–3D), indicating that etomidate injection induced motor deficits without anxiety-like behavior. We further analyzed the effect of etomidate on motor coordination. Etomidate injection induced a significant increase in the pole descent time (Figure 3E). These data establish a role of ZI in inducing bradykinesia and akinesia, and disrupting motor coordination, mimicking the motor deficits induced by 6-OHDA.

We next infused the GABA_A receptor antagonist bicuculline (5 μ g/ μ L, 1 μ L) into the ZI of 6-OHDA-treated mice. Compared with the NS naive mice, the 6-OHDA+NS group had a decreased balance beam score and an increased climbing time in the pole test. In addition, bicuculline injection into the ZI alleviated 6-OHDA-induced motor dysfunction (Figures 3F and 3G). These results indicated that pharmacological enhancement/suppression of the ZI GABAergic signaling affected motor behavior and parkinsonian signs.

Chemogenetic suppression of GABAergic neurons in the ZI induces parkinsonian motor symptoms in naive mice

The activity of GABAergic neurons in the ZI was modulated by the chemogenetic agents hM4D(Gi) and hM3D(Gq), which are DREADDs. pAAV-GAD67-hM4D(Gi)-mCherry-WPRE or pAAV-GAD67-hM3D(Gq)-mCherry-WPRE was injected into the ZI to inhibit or activate ZI GABAergic neurons, respectively. pAAV-GAD67-MCS- mCherry-3Flag was used as the control virus.

Inhibitory hM4D(Gi) and control virus were first injected into the ZI unilaterally or bilaterally. The schematic diagrams of the experiments are shown in Figures 4A and 4B. Behavioral tests were performed at least

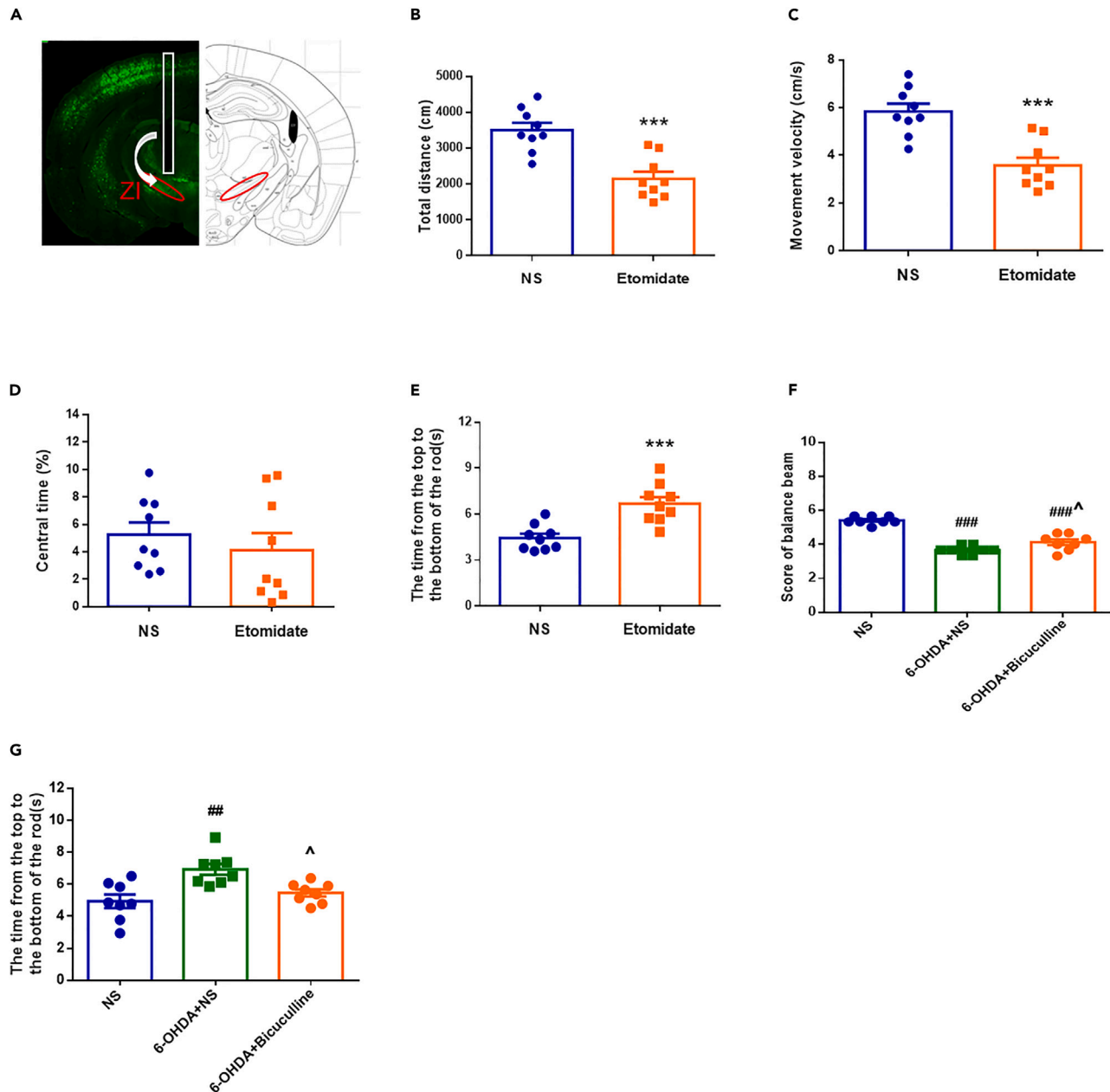


Figure 3. Microinjection of etomidate and/or bicuculline into the ZI regulates the motor performance in mice

(A) Illustration showing the implantation of the cannula.

(B–D) Performance of microinjection of the GABA_A receptor agonist etomidate into the ZI in the open-field test in naive mice: total movement distance (B), movement velocity (C), center zone exploration time (D). Etomidate injection mimicked the motor deficits induced by 6-OHDA in the naive mice.

(E) Microinjection of etomidate into the ZI increased the climbing time from the top to the bottom of the rod in the pole test.

(F) The balance beam score was decreased in the 6-OHDA+NS group compared with the NS group. Microinjection of the GABA_A receptor antagonist bicuculline into the ZI improved balance beam scores in 6-OHDA-lesioned mice.

(G) The climbing time in the pole test was increased in the 6-OHDA+NS group compared with the NS group. The injection of bicuculline into the ZI shortened the climbing time in 6-OHDA-lesioned mice. Each value is represented as means ± SEM. All data were normally distributed. ****p* < 0.001, compared with NS group, unpaired t-test was used; ##*p* < 0.01, ###*p* < 0.001, compared with NS group, ^*p* < 0.05, compared with the 6-OHDA+NS group, one-way ANOVA test was used. *n* = 8–9.

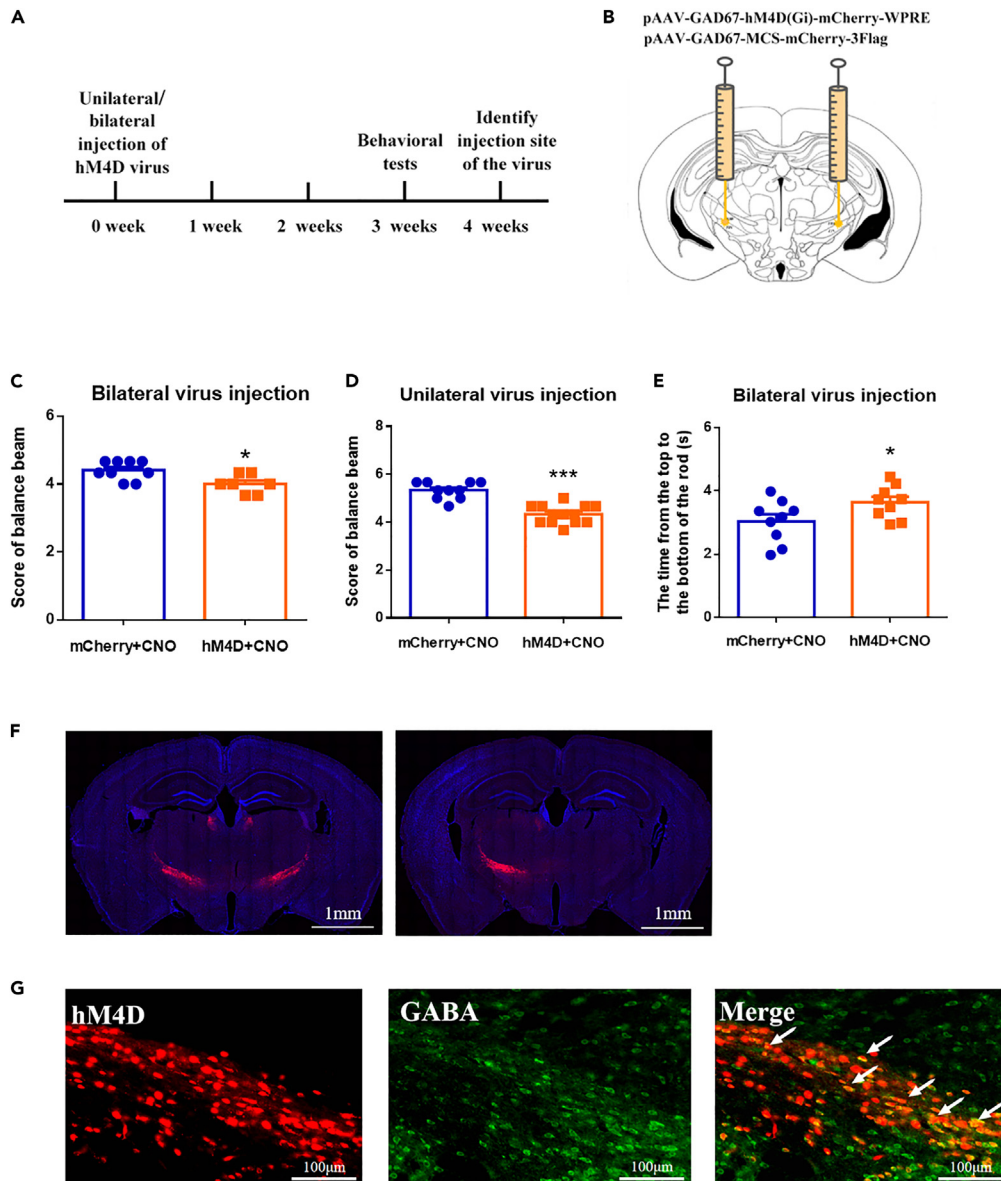


Figure 4. Chemogenetic inhibition of ZI GABAergic neurons induces parkinsonian motor symptoms in naive mice

(A and B) Schematics of pAAV-GAD67-hM4D(Gi)-mCherry-WPRE injection into the ZI unilaterally and/or bilaterally in naive mice.

(C and D) Bilateral and unilateral chemogenetic inhibition of the ZI GABAergic neurons by CNO decreased the balance beam score.

(E) Bilateral inhibition of the ZI GABAergic neurons by CNO increased the climbing time from the top to the bottom of the rod in the pole test.

(F) Chemogenetic virus expression in the ZI in coronal brain slices.

(G) GABAergic-positive cells were overlaid with hM4D-mCherry expression in the ZI. Each value is represented as means \pm SEM. All data were normally distributed, unpaired t-test was used, * $p < 0.05$, *** $p < 0.001$, compared with Control (mCherry+CNO), $n = 9-10$.

3 weeks after virus injection. The average scores of the control virus group and hM4D(Gi) group in the balance beam test after CNO injection were 5.33 and 4.33, respectively, suggesting that bilateral inhibition of GABAergic neurons with the DREADD hM4D(Gi) impaired the balance of naive mice (Figure 4C). Unilateral hM4D(Gi) virus injection produced similar results (Figure 4D). We also observed motor coordination changes in naive mice after bilateral virus injection. As shown in Figure 4E, compared with the control

mCherry virus group mice, the hM4D(Gi) group mice needed a longer time to climb from the top to the bottom in the pole test. The injection site and hM4D(Gi) virus expression in GABAergic neurons were confirmed by histological studies at the end of the experiments (Figures 4F and 4G). Together, these results indicated that chemogenetic inhibition of ZI GABAergic neurons in naive mice induced parkinsonian motor symptoms.

Chemogenetic activation of ZI GABAergic neurons attenuates motor dysfunction in 6-OHDA-induced PD model mice

As we showed that chemogenetic inhibition of ZI GABAergic neurons induced parkinsonian motor symptoms, we speculated that activation of these neurons could rescue motor deficits. Figure 5A shows a schematic diagram of the experiment. 6-OHDA was injected unilaterally into the striatum, and hM3D(Gq) or control virus was injected into the ipsilateral ZI (Figure 5B). 6-OHDA and the viral vectors were injected during the same procedure. Two weeks after the 6-OHDA injection, the APO-induced rotation number was determined to evaluate the success of a hemi-parkinsonian model establishment.

As expected, after three weeks of virus expression, activation of hM3D(Gq) by CNO rescued motor dysfunction in PD mice. In these experiments, 6-OHDA-lesioned PD mice expressing hM3D in the ZI were intraperitoneally injected with CNO or NS in a blinded manner. We also compared the effects of CNO and NS in 6-OHDA-treated mice injected with the control mCherry virus. Specifically, the total distance traveled and velocity significantly increased in the CNO-treated hM3D PD group compared with the NS-treated PD group (Figures 5C–5E). ZI GABAergic neuron activation did not affect the central zone exploration time (Figure 5F). Moreover, chemogenetic activation of ZI GABAergic neurons improved the balance of PD mice (Figure 5G). We also used the CatWalk system to assess gait disturbance. The base of support of the front paws was analyzed. As shown in Figure 5H, there was no difference between 6-OHDA-treated control mCherry virus-expressing mice in the NS group and those in the CNO group. However, hM3D activation by CNO decreased the base of support in 6-OHDA-treated mice. The virus injection site and hM3D expression were confirmed, as shown in Figures 5I and 5J.

The effects of repeated hM3D-mediated activation of ZI GABAergic neurons on motor behaviors and the nigrostriatal system in 6-OHDA-induced PD model mice

The above experiments tested the effects of acute CNO-mediated activation of hM3D on motor behaviors. We next evaluated the effect of repeated CNO injections. The schematic diagrams of the experiments are shown in Figures 6A and 6B. Three weeks after 6-OHDA lesioning and virus injection, mice received daily injections of CNO for 7 days. Then, motor behaviors were tested using the open-field test, the balance beam test, the pole test, and gait analysis. Similar to our previous results, repeated activation of hM3D alleviated the decrease in locomotion and impairment of balance and motor coordination in PD mice (Figures 6C–6G). Gait analysis also showed that continuous CNO injection increased the maximum contact area, print length, print width, and print area (Figures 6H–6K). We further measured catecholamine content in the striatum. Repeated activation of hM3D in 6-OHDA-treated mice increased the tissue levels of DA and its metabolites DOPAC and HVA (Figures 6L–6M).

Optogenetic suppression of GABAergic neurons in the ZI induces parkinsonian motor symptoms in naive mice

We next suppressed the activity of GABAergic neurons in the ZI using the optogenetic agent eNpHR. pAAV-GAD67-eNpHR3.0-EGFP-3xFLAG-WPRE was injected into the ZI unilaterally or bilaterally to inhibit GABAergic neurons. pAAV-GAD67-EGFP-3xFLAG-WPRE was used as the control virus. Schematic diagrams of the experiments are shown in Figures 7A and 7B.

In the open-field test, during light stimulation (unilateral), the NpHR group showed decreases in the total distance traveled and velocity. The EGFP control group showed no significant change in movement parameters during light stimulation compared with the light-off state (Figures 7C–7E). All mice in the NpHR and control groups had similar scores in the balance beam test in the light-off state. During light stimulation, the balance score decreased from 5.5 to 4.4 in the NpHR group (Figure 7F). Bilateral inhibition of GABAergic neurons with NpHR also resulted in parkinsonian movement symptoms (Figures 7G–7J). The

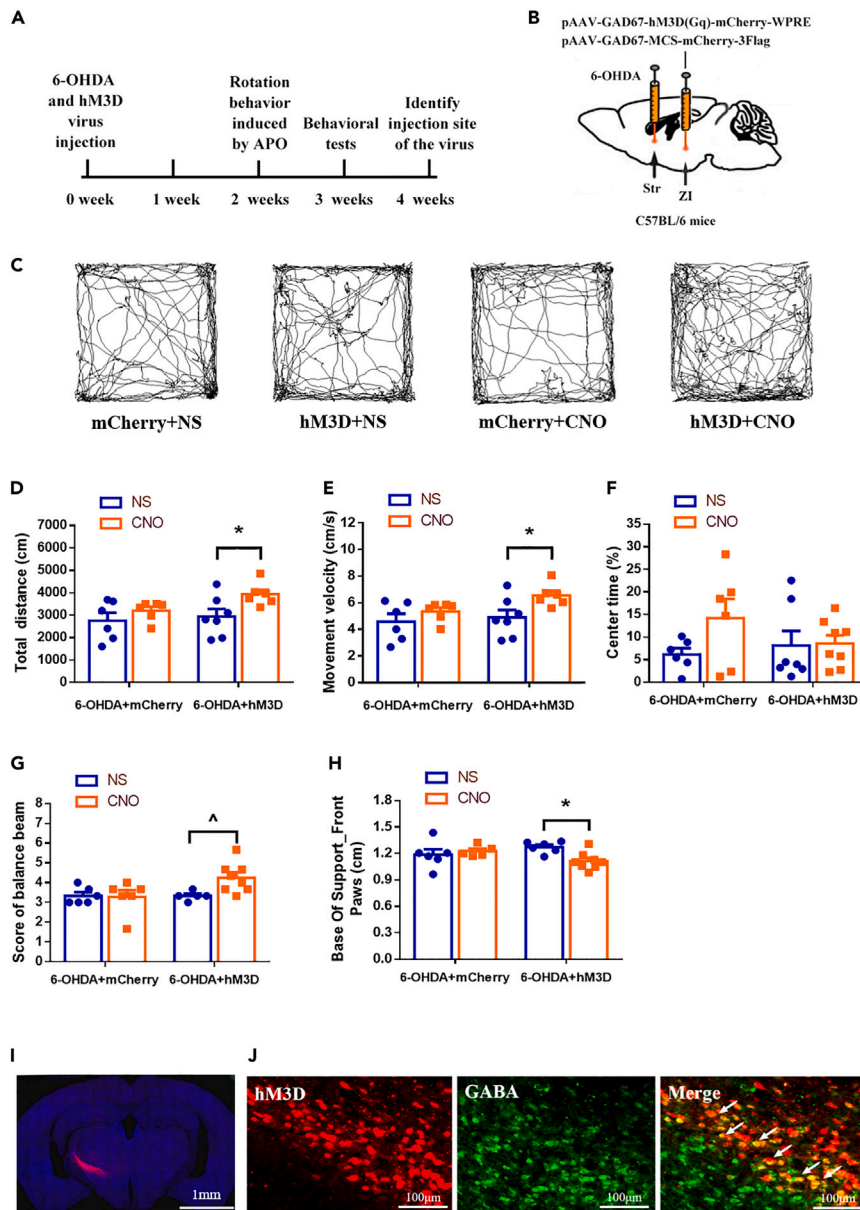


Figure 5. Chemogenetic activation of ZI GABAergic neurons ameliorates motor deficits in 6-OHDA-induced PD mice

(A and B) Schematics of pAAV-GAD67-hM3D(Gq)-mCherry-WPRE injection into the ZI unilaterally in 6-OHDA-induced PD mice.

(C) Sample track maps in the open-field test after application of NS and CNO in 6-OHDA-induced PD mice expressing hM3D and/or mCherry control virus in the ZI.

(D–F) Performance of PD mice expressing hM3D and/or mCherry control virus and treated with NS and CNO, respectively, in the open-field test: total movement distance (D), velocity (E), and center time (F).

(G) The scores of PD mice expressing hM3D and/or mCherry control virus and treated with NS and CNO, respectively, in the balance beam test.

(H) Gait analysis showed the base of support-front paws in different groups treated with NS and CNO, respectively.

(I) Chemogenetic virus expression in the ZI in coronal brain slices. (J) GABAergic-positive cells were overlaid with hM3D-mCherry expression in the ZI. Each value is represented as means \pm SEM. Data in (D), (E), and (H) showed normal distribution, two-way ANOVA was used, * $p < 0.05$, compared with mCherry+CNO group; # $p < 0.05$, compared with hM3D + NS group, $n = 6-8$. Data in (G) and (F) showed nonnormal distribution, non-parametric test was used, ^ $p < 0.05$, compared with hM3D + NS group, $n = 6-8$.

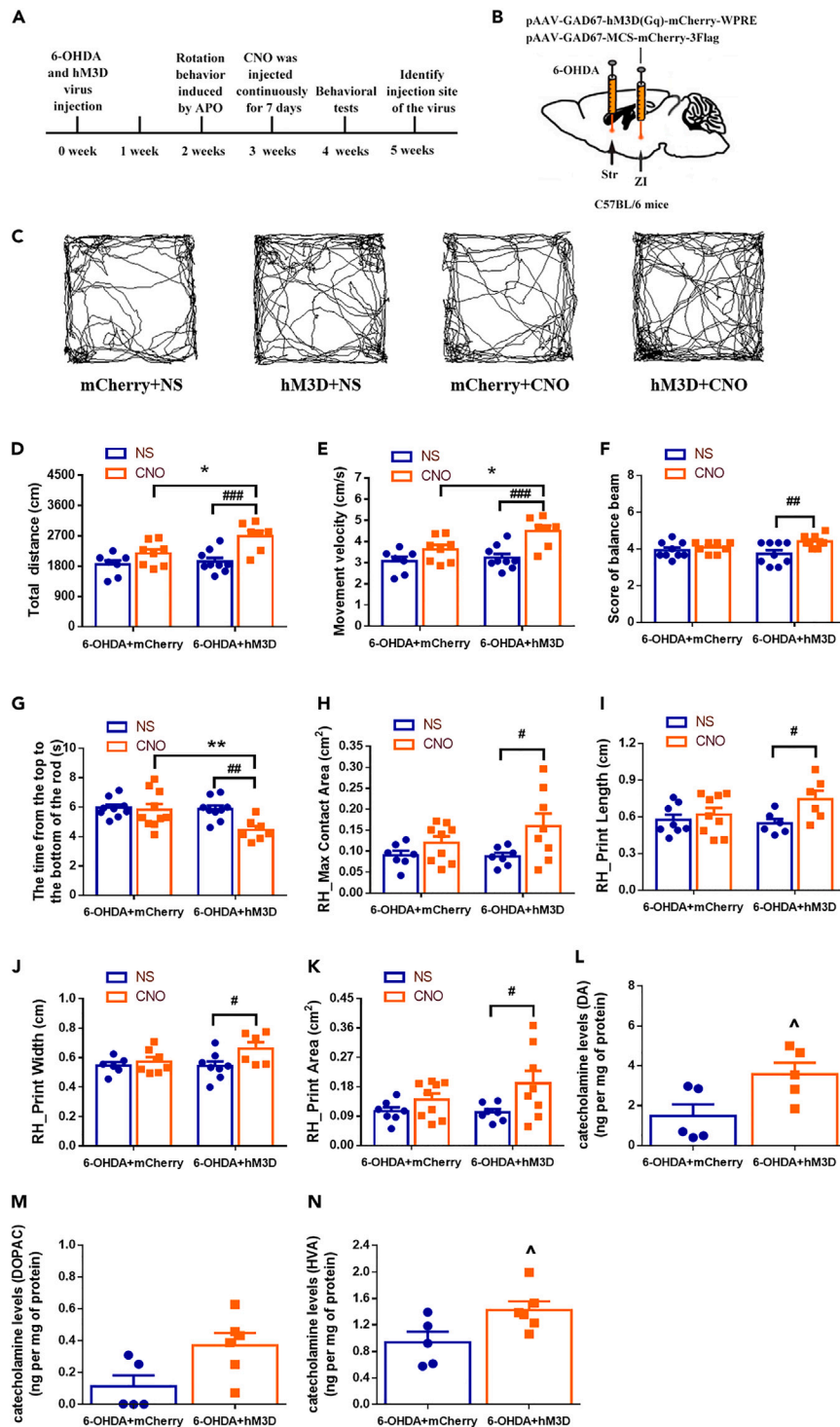


Figure 6. Extended activation of ZI GABAergic neurons by repeated CNO application

(A and B) Schematics of pAAV-GAD67-hM3D(Gq)-mCherry-WPRE injection into the ZI unilaterally in 6-OHDA-induced PD mice. Mice were treated with CNO and/or NS once daily for 7 days.

(C) Sample track maps in the open-field test after application of 7 CNO and NS in 6-OHDA-induced PD mice expressing hM3D and/or mCherry control virus in the ZI.

(D and E) Performance of PD mice expressing hM3D and/or mCherry control virus and treated with NS and CNO continuously in the open-field test: total movement distance (D), and velocity (E).

Figure 6. Continued

(F) The scores of PD mice expressing hM3D and/or mCherry control virus and treated with CNO and NS continuously in the balance beam test.

(G) The climbing time from the top to the bottom of the rod in different groups after CNO and NS treatment.

(H–K) Gait analysis showed the max contact area (H), print length (I), print width (J), and print area (K) in different groups treated with CNO and NS continuously in different groups.

(L) Extended activation of the ZI GABAergic neurons by repeated CNO application in 6-OHDA-induced PD mice increased the contents of DA and its two metabolites DOPAC and HVA in the striatum. Each value is represented as means \pm SEM. For all behavioral tests, two-way ANOVA was used, * $p < 0.05$, ** $p < 0.01$, compared with mCherry+CNO group; # $p < 0.05$, ## $p < 0.01$, ### $p < 0.001$, compared with hM3D + NS group, $n = 8–10$; For HPLC test, unpaired t-test was used, ^ $p < 0.05$, compared with the 6-OHDA+mCherry group; data in (M) showed nonnormal distribution, non-parametric test was used, $n = 5–6$.

virus injection site and NpHR expression in ZI GABAergic neurons were confirmed, as shown in [Figures 7K](#) and [7L](#).

Optogenetic activation of ZI GABAergic neurons attenuates motor dysfunction in 6-OHDA-induced PD model mice

To test whether optogenetic GABAergic neuron activation can attenuate motor impairment in PD mice, we injected mice with the Chr2 virus. We first injected 6-OHDA into the striatum unilaterally and/or bilaterally. Immediately after 6-OHDA infusion, pAAV-GAD67-hChr2(H134R)-EGFP-3xFLAG-WPRE or control virus was injected into the ZI ([Figures 8A](#) and [8B](#)). Similar to the results of our previous chemogenetic experiment, unilateral light stimulation of ZI GABAergic neurons significantly ameliorated motor deficits in PD mice. In the open-field test, the total distance traveled increased from 1244 in the light-off state to 1560 cm during light stimulation in the Chr2 group. No change was observed in the control EGFP virus group ([Figures 8C](#) and [8D](#)). Light stimulation also increased the movement velocity but did not affect the time spent in the central area ([Figures 8E](#) and [8F](#)). Moreover, bilateral activation of ZI GABAergic neurons in bilaterally lesioned PD mice attenuated motor dysfunction ([Figures 8G–8I](#)).

Finally, we repeated the above experiments with Vgat-Cre mice to further clarify the role of ZI GABAergic neurons in the regulation of PD motor behavior. The PD model was prepared by injecting 6-OHDA into the striatum of Vgat-Cre mice. Meanwhile, the activated optogenetic virus pAAV-EF1a-DIO-hChr2(H134R)-mCherry or the control virus pAAV-EF1a-DIO-mCherry-WPRE was injected into the ZI on the same side ([Figure 8J](#)). Similarly, light stimulation of the ZI GABAergic neurons in Vgat-Cre mice significantly improved the movement behavior of PD mice ([Figures 8K–8N](#)). The results showed that compared with the mCherry control group, the total distance and velocity of Chr2 group were significantly increased during light stimulation. The virus injection site and the expression of Chr2 were verified in [Figures 8O](#) and [8P](#). Taken together, these findings demonstrated that the ZI GABAergic neurons activation ameliorated a series of motor deficits in the 6-OHDA mouse model of PD.

DISCUSSION

In the present study, we identified a critical role of ZI GABAergic neurons in models of parkinsonism. Unilateral and/or bilateral injection of 6-OHDA into the striatum caused damage to the substantia nigra. Furthermore, chemogenetic and optogenetic stimulation of ZI GABAergic neurons improved the motor performance of mice. To the best of our knowledge, we are the first to report on the beneficial effects of ZI GABAergic neuron manipulation in experimental PD.

In the first part of our experiment, we sought to confirm the neurotoxic effects of 6-OHDA on the nigrostriatal system and explore whether neurons in the ZI were damaged. Since it was first described in 1959, 6-OHDA has become one of the most widely used neurotoxins for modeling PD in experimental animals.^{24,25} Because of the difficulty in targeting the SNc and medial forebrain bundle due to their small size, 6-OHDA was previously more commonly used in rats than in mice to model PD.³¹ However, with the development of novel chemogenetic and optogenetic tools, the construction of transgenic mice, 6-OHDA began to be stereotactically injected into large structures such as the striatum in mice.^{26,32–34} When delivered to this region, 6-OHDA induces slow, progressive, and partial damage to the substantia nigra in a retrograde fashion over a period of up to 2 or 3 weeks. In this model, we observed that striatal

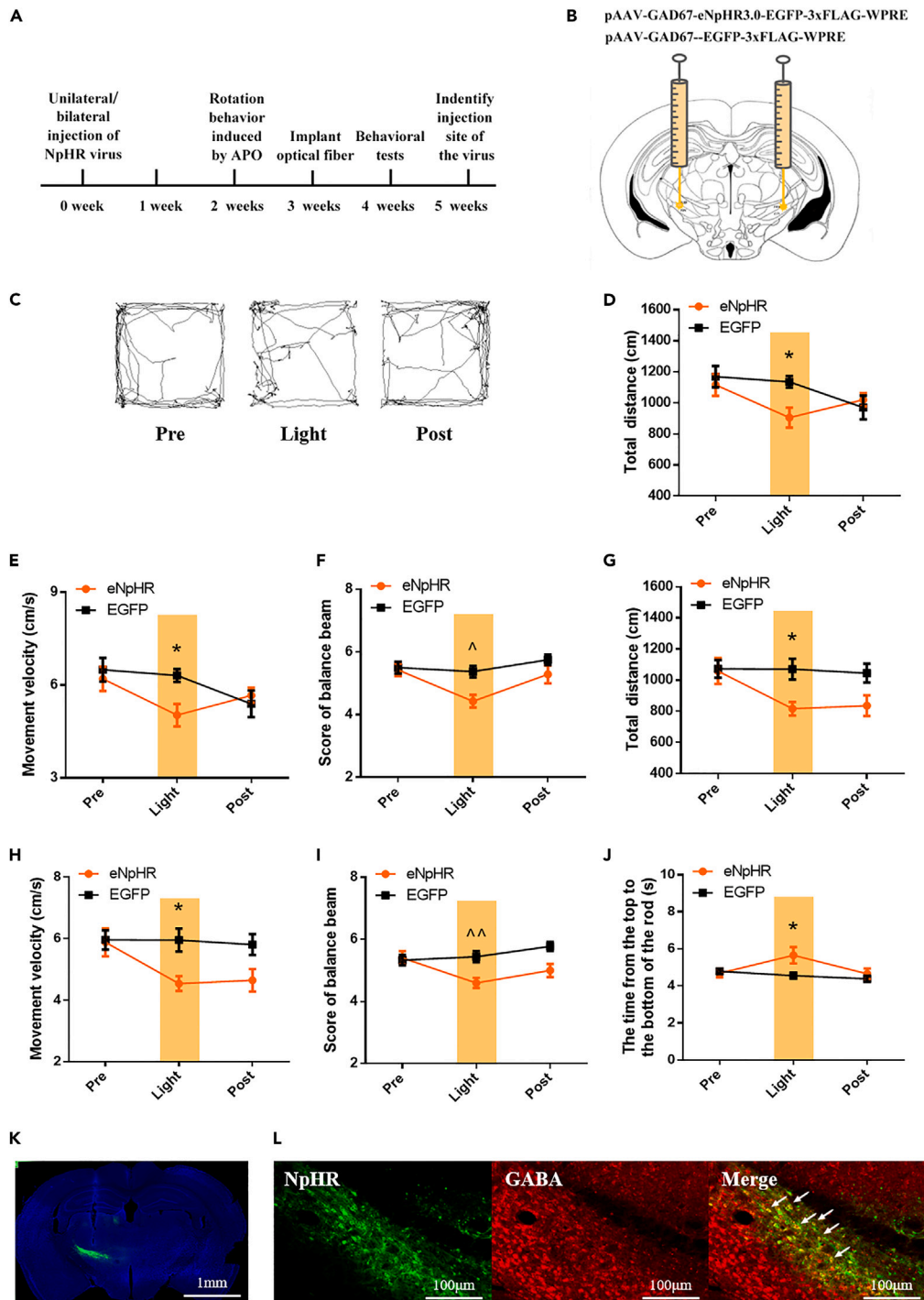


Figure 7. Optogenetic inhibition of the ZI GABAergic neurons induces parkinsonian motor symptoms in naive mice

(A and B) Schematics of pAAV-GAD67-eNpHR3.0-EGFP-3xFLAG-WPRE injection into the ZI unilaterally or bilaterally in naive mice.

(C) Sample track maps in the open-field test during Pre-Light-Post trials in naive mice expressing NpHR unilaterally in the ZI.

(D and E) Performance of naive mice expressing NpHR unilaterally in the open-field test: total movement distance (D), and velocity (E) during Pre-Light-Post trials.

(F) The scores of naive mice expressing NpHR unilaterally in the balance beam test during Pre-Light-Post trials.

Figure 7. Continued

(G and H) Performance of naive mice expressing NpHR bilaterally in the open-field test: total movement distance (G), and velocity (H) during Pre-Light-Post trials.

(I) The scores of naive mice expressing NpHR bilaterally in the balance beam test during Pre-Light-Post trials.

(J) The climbing time from the top to the bottom of the rod of naive mice expressing NpHR bilaterally in the pole test during Pre-Light-Post trials.

(K) NpHR-EGFP expression in the ZI.

(L) GABAergic-positive cells were overlaid with NpHR-EGFP expression in the ZI. Each value is represented as means \pm SEM. Data in (D), (E), (G), (H) and (I) showed normal distribution, two-way ANOVA was used, $*p < 0.05$, $n = 7-10$. Data in (F) and (J) showed nonnormal distribution, non-parametric test was used, $^{\wedge}p < 0.05$, $^{\wedge\wedge}p < 0.01$, $n = 7-10$.

6-OHDA injection significantly decreased the number of TH⁺ fibers in the striatum and the number of TH⁺ cells in the SNc. We then assessed locomotor activity in the open-field test and found decreases in total distance traveled and movement velocity in 6-OHDA-lesioned mice compared with NS-treated control mice. The balance beam and pole tests further demonstrated loss of balance and impaired motor coordination. Our next goal was to determine whether there was any pathological change in ZI. Previous studies reported an overall 50% reduction in the number of PV⁺ neurons in the ZI at 3 to 84 days after 6-OHDA lesioning in rats.²⁹ Similarly, in the present study, striatal 6-OHDA injection decreased the number of GABA⁺ and PV⁺ neurons in mice compared with NS injection. In summary, these results suggest that the expression of neurotransmitters in the ZI is altered after 6-OHDA lesioning. Further studies are needed to explore the factors that trigger these changes.

The second part of this study involved modulation of PD motor symptoms using pharmacological, chemogenetic, and optogenetic approaches. As PD is primarily considered a motor disorder, the diagnosis of PD often relies on the presence of a set of motor symptoms, such as bradykinesia, rest tremor, and muscular rigidity. As PD progresses, gait disturbance and postural instability become increasingly prominent. The ZI has been reported to be involved in movement behavior. As early as the 1950s, Grossman et al. found that stimulation of the medial portion of the ZI elicited walking movements in anesthetized cats.³⁵ In rats, administration of bicuculline into the ZI was found to reduce the haloperidol-induced parkinsonian catalepsy, whereas injection of muscimol, an agonist of GABA_A receptors, evoked severe catalepsy that resembled that induced by haloperidol.³⁶ Microinjection of bicuculline into the ZI also induced an increase in locomotion.³⁷ We also observed that bicuculline infusion rescued 6-OHDA-induced motor impairments. However, these pharmacological data cannot suggest a real contribution of the GABAergic neurons to the parkinsonian motor symptoms. Chemogenetic/optogenetic-based treatments are reversible, better controlled, and directly increase or inhibit neuronal excitability. Here, we found significant improvement of motor function in PD model mice by chemogenetic/optogenetic activation of GABAergic neurons within the ZI. The present study not only evaluated the acute effect of stimulation of GABAergic neurons on motor performance but also assessed the effect of repeated activation on the nigrostriatal system by CNO. Similar to a single dose of CNO, repeated activation of DREADDs improved motor performance. More importantly, the striatal DA content was increased. For the first time, we confirmed the role of GABAergic neurons in the ZI in PD motor symptoms.

Although the potential mechanisms remain unclear, several factors might suggest the contribution of the ZI GABAergic neurons to the parkinsonian condition. First, the extensive inter-connections within the ZI were evidenced before. According to Power et al., the cells in a particular ZI sector could influence the activity of nearby cells in the same sector and more distant cells in other sectors.^{9,38} They injected biotinylated dextran into each of the four ZI sectors (ZIr, ZId, ZIv, and ZIc) and examined the patterns of labeling across the ipsilateral and contralateral ZI. They observed that after such injections (into each sector), many labeled terminals were found throughout the ZI of the ipsilateral and the contralateral side. At present, our results showed that stimulation of ZI GABAergic neurons ameliorated the parkinsonian motor deficits, and Li et al. recently found that glutamatergic neurons in the ZIc were hyperactive in mouse models of PD, and inhibition of their activity ameliorated the motor deficits.³⁹ It is possible that GABAergic neurons in the ZI modulate the activity of local glutamatergic cells. If so, both the chemogenetic/optogenetic stimulation of GABAergic neurons in the present study and optogenetic inhibition of glutamatergic neurons in Li's study rescued the parkinsonian motor symptoms. Further studies are needed to examine the intrinsic incerto-incertal GABAergic-glutamatergic connections in mice. Second, the multiple input-output connections of the ZI GABAergic neurons

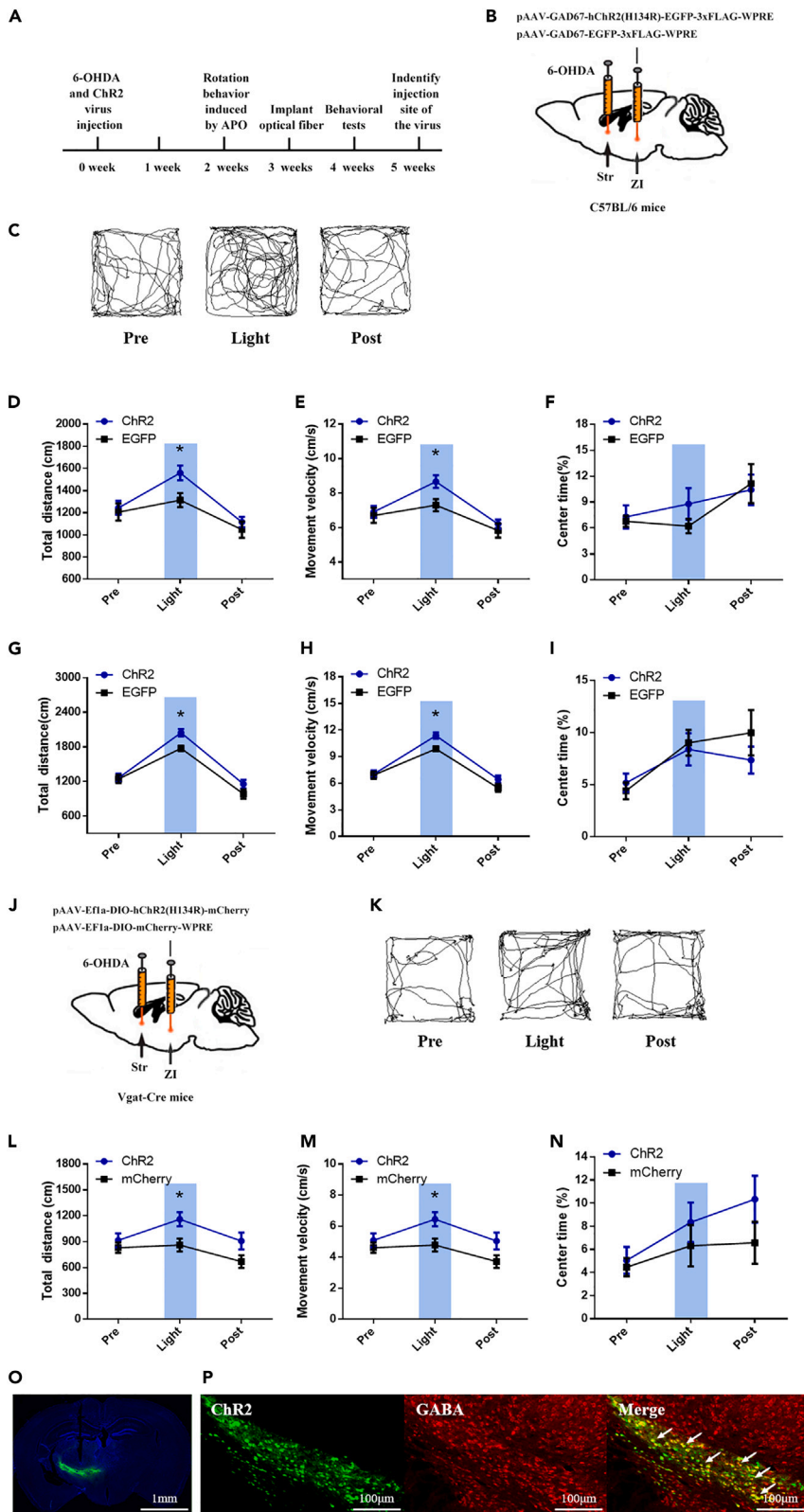


Figure 8. Optogenetic activation of the ZI GABAergic neurons ameliorates motor deficits in 6-OHDA-induced PD mice

(A and B) Schematics of pAAV-GAD67-hChr2(H134R)-EGFP-3xFLAG-WPRE injection into the ZI unilaterally or bilaterally in 6-OHDA-induced PD mice.
 (C) Sample track maps in the open-field test during Pre-Light-Post trials in 6-OHDA-induced PD mice expressing Chr2 unilaterally in the ZI.
 (D–F) Performance of PD mice expressing Chr2 unilaterally in the open-field test: total movement distance (D), velocity (E) and time spent in the central area (F) during Pre-Light-Post trials.
 (G–I) Performance of PD mice expressing Chr2 bilaterally in the open-field test: total movement distance (G), velocity (H) and time spent in the central area (I) during Pre-Light-Post trials.
 (J) Schematics of pAAV-EF1a-DIO-mCherry-WPRE, pAAV-EF1a-DIO-hChr2(H134R)-mCherry and 6-OHDA injection in the Vgat-Cre mice.
 (K) Sample track maps in the open-field test during Pre-Light-Post trials.
 (L–N) Performance of PD mice (Vgat-Cre mice) expressing Chr2 unilaterally in the open-field test: total movement distance (L), velocity (M) and time spent in the central area (N) during Pre-Light-Post trials.
 (O) Chr2-EGFP expression in the ZI. (P) GABAergic-positive cells were overlaid with Chr2-EGFP expression in the ZI. Each value is represented as means \pm SEM. Data in (F) showed nonnormal distribution, non-parametric test was used, other data are in line with normal distribution, two-way ANOVA was used, * $p < 0.05$, $n = 11–14$.

facilitate global behavioral modulation. All sectors of the ZI send fibers to the basal ganglia structures (substantia nigra, globus pallidus). Moreover, afferents from the substantia nigra and other brainstem nuclei (midbrain reticular nucleus, pontine reticular nucleus, ventral tegmental area, tegmental pedunculo-pontine nucleus, dorsal raphe, periaqueductal gray matter) terminate in the ZI.^{7,9,15,40} Based on these anatomical data, the ZI is an essential link in a neuronal chain transmitting impulses involved in PD pathology.

Clinically, ZI has been implicated in alleviating motor symptoms in treatments of PD using DBS. ZI is traversed by fibers of pallidothalamic, nigrothalamic, and cerebellothalamic projections which convey pathological impulses involved in the generation of bradykinesia, muscle rigidity, and tremor.^{41–43} Therefore, it cannot be excluded that stimulation of these fibers by DBS is the cause of amelioration of these signs. However, our present results and Li's study³⁹ suggested that, besides fibers passing through, neurons of the ZI may also be important for the treatment of PD.

In the present study, we exclusively focused on the association of ZI activity with movement. Future studies could explore the role of the ZI as a target for the treatment of nonmotor PD symptoms, such as sleep disorders, pain, anxiety, and depression, and the underlying cellular mechanisms.⁴⁴ The ZI has already been implicated in related processes. For example, Lhx6-positive GABA-releasing neurons in the ZI have been found to promote sleep.⁴⁵ It was found that optogenetic manipulation of the two GABAergic subpopulations in the ZI, i.e., somatostatin- and calretinin-expressing neurons, triggers specific anxiety-related behavioral phenotypes.¹² Moreover, clinical reports have found that DBS of the ZI leads to a decrease in self-reported anxiety and depression and an improvement in fear recognition in PD patients.⁴⁶ ZI DBS at 130 Hz was found to decrease perceived thermal pain in PD patients, and low-frequency stimulation at 20 Hz also reduced pain elicited by heat.²⁰

In conclusion, the results of our present study reveal the function of ZI GABAergic neurons in 6-OHDA-lesioned PD mouse models. Activation of these neurons using chemogenetics and optogenetics may effectively improve motor function. These findings suggest the potential role of ZI GABAergic neurons as targets for the treatment of PD.

Limitations of the study

In this study, we found that the ZI GABAergic neurons played an important role in PD motor dysfunction. Chemogenetic/optogenetic activation of these neurons alleviated locomotion deficits in 6-OHDA-induced PD mice. In addition, we also found that repeated chemogenetic activation of ZI GABAergic neurons by CNO increased the dopamine content in the striatum. To the best of our knowledge, we are the first to report on the beneficial effects of chemogenetic and optogenetic manipulations of the ZI GABAergic neurons in experimental PD. But the underlying mechanisms remain unknown. Future work should be carried out to elucidate the functional and circuit-level connections of the incertal GABAergic pathway.

STAR★METHODS

Detailed methods are provided in the online version of this paper and include the following:

- **KEY RESOURCES TABLE**
- **RESOURCE AVAILABILITY**
 - Lead contact
 - Materials availability
 - Data and code availability
- **EXPERIMENTAL MODEL AND STUDY PARTICIPANT DETAILS**
 - Animals
 - Establishment of the 6-OHDA model
 - Cannula implantation
 - Virus injection
- **METHOD DETAILS**
 - Optogenetic manipulation
 - Chemogenetic manipulation
 - Rotation test
 - Open-field test
 - Rotarod test
 - Pole test
 - Balance beam test
 - Gait analysis
 - Immunofluorescence staining
 - High-performance liquid chromatography (HPLC) with electrochemical detection
- **QUANTIFICATION AND STATISTICAL ANALYSIS**
 - Statistical analysis

ACKNOWLEDGMENTS

This work was funded by the National Natural Science Foundation of China (32171132 and 32170984), the Shandong Provincial Natural Science Foundation (ZR2021MC167), the Postdoctoral Science Foundation of China (2017M610412 and 2018T110666), and Taishan Scholars Construction Project.

AUTHOR CONTRIBUTIONS

F.C. performed the chemogenetic and optogenetic experiments; J.Q. performed the optogenetic experiments; Z.C. performed the pharmacological experiments; A.L. helped to do the immunostaining tests; J.C. helped to do some behavior tests. L.S. conceived the study, wrote the original draft of the manuscript, and provided funding support. J.X. revised, finalized the manuscript, and provided funding support. All authors read and approved the final manuscript.

DECLARATION OF INTERESTS

The authors declare no competing interests.

Received: January 17, 2023

Revised: April 26, 2023

Accepted: June 12, 2023

Published: June 15, 2023

REFERENCES

1. Poewe, W., Seppi, K., Tanner, C.M., Halliday, G.M., Brundin, P., Volkman, J., Schrag, A.E., and Lang, A.E. (2017). Parkinson disease. *Nat. Rev. Dis. Primers* 3, 17013. <https://doi.org/10.1038/nrdp.2017.13>.
2. Kalia, L.V., and Lang, A.E. (2015). Parkinson's disease. *Lancet* 386, 896–912. [https://doi.org/10.1016/S0140-6736\(14\)61393-3](https://doi.org/10.1016/S0140-6736(14)61393-3).
3. Obeso, J.A., Stamelou, M., Goetz, C.G., Poewe, W., Lang, A.E., Weintraub, D., Burn, D., Halliday, G.M., Bezard, E., Przedborski, S., et al. (2017). Past, present, and future of Parkinson's disease: A special essay on the 200th Anniversary of the Shaking Palsy. *Mov. Disord.* 32, 1264–1310. <https://doi.org/10.1002/mds.27115>.
4. Elkouzi, A., Vedam-Mai, V., Eisinger, R.S., and Okun, M.S. (2019). Emerging therapies in Parkinson disease - repurposed drugs and new approaches. *Nat. Rev. Neurol.* 15, 204–223. <https://doi.org/10.1038/s41582-019-0155-7>.
5. Lee, D.J., and Lozano, A.M. (2018). The Future of Surgical Treatments for Parkinson's Disease. *J. Parkinsons Dis.* 8, S79–S83. <https://doi.org/10.3233/JPD-181467>.

6. Baumgartner, A.J., Thompson, J.A., Kern, D.S., and Ojemann, S.G. (2022). Novel targets in deep brain stimulation for movement disorders. *Neurosurg. Rev.* 45, 2593–2613. <https://doi.org/10.1007/s10143-022-01770-y>.
7. Yang, Y., Jiang, T., Jia, X., Yuan, J., Li, X., and Gong, H. (2022). Whole-Brain Connectome of GABAergic Neurons in the Mouse Zona Incerta. *Neurosci. Bull.* 38, 1315–1329. <https://doi.org/10.1007/s12264-022-00930-w>.
8. Wang, X., Chou, X.L., Zhang, L.I., and Tao, H.W. (2020). Zona Incerta: An Integrative Node for Global Behavioral Modulation. *Trends Neurosci.* 43, 82–87. <https://doi.org/10.1016/j.tins.2019.11.007>.
9. Mitrofanis, J. (2005). Some certainty for the "zone of uncertainty"? Exploring the function of the zona incerta. *Neuroscience* 130, 1–15. <https://doi.org/10.1016/j.neuroscience.2004.08.017>.
10. de Git, K.C.G., Hazelhoff, E.M., Nota, M.H.C., Schele, E., Luijendijk, M.C.M., Dickson, S.L., van der Plasse, G., and Adan, R.A.H. (2021). Zona incerta neurons projecting to the ventral tegmental area promote action initiation towards feeding. *J. Physiol.* 599, 709–724. <https://doi.org/10.1113/JP276513>.
11. Venkataraman, A., Hunter, S.C., Dhinojwala, M., Ghebrezadik, D., Guo, J., Inoue, K., Young, L.J., and Dias, B.G. (2021). Incertothalamic modulation of fear via GABA and dopamine. *Neuropsychopharmacology* 46, 1658–1668. <https://doi.org/10.1038/s41386-021-01006-5>.
12. Li, Z., Rizzi, G., and Tan, K.R. (2021). Zona incerta subpopulations differentially encode and modulate anxiety. *Sci. Adv.* 7, eabf6709. <https://doi.org/10.1126/sciadv.abf6709>.
13. Hormigo, S., Zhou, J., and Castro-Alamancos, M.A. (2020). Zona Incerta GABAergic Output Controls a Signaled Locomotor Action in the Midbrain Tegmentum. *eNeuro* 7, ENEURO.0390-19.2020. <https://doi.org/10.1523/ENEURO.0390-19.2020>.
14. Venkataraman, A., Brody, N., Reddi, P., Guo, J., Gordon Rainnie, D., and Dias, B.G. (2019). Modulation of fear generalization by the zona incerta. *Proc. Natl. Acad. Sci. USA* 116, 9072–9077. <https://doi.org/10.1073/pnas.1820541116>.
15. Ossowska, K. (2020). Zona incerta as a therapeutic target in Parkinson's disease. *J. Neurol.* 267, 591–606. <https://doi.org/10.1007/s00415-019-09486-8>.
16. Plaha, P., Ben-Shlomo, Y., Patel, N.K., and Gill, S.S. (2006). Stimulation of the caudal zona incerta is superior to stimulation of the subthalamic nucleus in improving contralateral parkinsonism. *Brain* 129, 1732–1747. <https://doi.org/10.1093/brain/awl127>.
17. Stenmark Persson, R., Nordin, T., Hariz, G.M., Wårdell, K., Forsgren, L., Hariz, M., and Blomstedt, P. (2022). Deep Brain Stimulation of Caudal Zona Incerta for Parkinson's Disease: One-Year Follow-Up and Electric Field Simulations. *Neuromodulation* 25, 935–944. <https://doi.org/10.1111/ner.13500>.
18. Sundstedt, S., Holmén, L., Rova, E., Linder, J., Nordh, E., and Olofsson, K. (2017). Swallowing safety in Parkinson's disease after zona incerta deep brain stimulation. *Brain Behav.* 7, e00709. <https://doi.org/10.1002/brb3.709>.
19. Philipson, J., Blomstedt, P., Fredricks, A., Hariz, M., Stenmark Persson, R., and Jahanshahi, M. (2021). Short- and long-term cognitive effects of deep brain stimulation in the caudal zona incerta versus best medical treatment in patients with Parkinson's disease. *J. Neurosurg.* 134, 357–365. <https://doi.org/10.3171/2019.12.JNS192654>.
20. Lu, C.W., Harper, D.E., Askari, A., Willsey, M.S., Vu, P.P., Schrepf, A.D., Harte, S.E., and Patil, P.G. (2021). Stimulation of zona incerta selectively modulates pain in humans. *Sci. Rep.* 11, 8924. <https://doi.org/10.1038/s41598-021-87873-w>.
21. Ordaz, J.D., Wu, W., and Xu, X.M. (2017). Optogenetics and its application in neural degeneration and regeneration. *Neural Regen. Res.* 12, 1197–1209. <https://doi.org/10.4103/1673-5374.213532>.
22. Assaf, F., and Schiller, Y. (2019). A chemogenetic approach for treating experimental Parkinson's disease. *Mov. Disord.* 34, 469–479. <https://doi.org/10.1002/mds.27554>.
23. Duty, S., and Jenner, P. (2011). Animal models of Parkinson's disease: a source of novel treatments and clues to the cause of the disease. *Br. J. Pharmacol.* 164, 1357–1391. <https://doi.org/10.1111/j.1476-5381.2011.01426.x>.
24. Salari, S., and Bagheri, M. (2019). In vivo, in vitro and pharmacologic models of Parkinson's disease. *Physiol. Res.* 68, 17–24. <https://doi.org/10.33549/physiolres.933895>.
25. Simola, N., Morelli, M., and Carta, A.R. (2007). The 6-hydroxydopamine model of Parkinson's disease. *Neurotox. Res.* 11, 151–167. <https://doi.org/10.1007/BF03033565>.
26. Zhang, H., Zhang, C., Qu, Z., Li, B., Su, Y., Li, X., Gao, Y., and Wang, Y. (2021). STN-ANT plasticity is crucial for the motor control in Parkinson's disease model. *Signal Transduct. Target. Ther.* 6, 215. <https://doi.org/10.1038/s41392-021-00545-z>.
27. Feeney, D.M., Gonzalez, A., and Law, W.A. (1982). Amphetamine, haloperidol, and experience interact to affect rate of recovery after motor cortex injury. *Science* 217, 855–857. <https://doi.org/10.1126/science.7100929>.
28. Li, J., Bai, Y., Liang, Y., Zhang, Y., Zhao, Q., Ge, J., Li, D., Zhu, Y., Cai, G., Tao, H., et al. (2022). Parvalbumin Neurons in Zona Incerta Regulate Itch in Mice. *Front. Mol. Neurosci.* 15, 843754. <https://doi.org/10.3389/fnmol.2022.843754>.
29. Heise, C.E., and Mitrofanis, J. (2005). Reduction in parvalbumin expression in the zona incerta after 6OHDA lesion in rats. *J. Neurocytol.* 34, 421–434. <https://doi.org/10.1007/s11068-006-8728-y>.
30. Jiang, H., Li, L.J., Wang, J., and Xie, J.X. (2008). Ghrelin antagonizes MPTP-induced neurotoxicity to the dopaminergic neurons in mouse substantia nigra. *Exp. Neurol.* 212, 532–537. <https://doi.org/10.1016/j.expneurol.2008.05.006>.
31. Tieu, K. (2011). A guide to neurotoxic animal models of Parkinson's disease. *Cold Spring Harb. Perspect. Med.* 1, a009316. <https://doi.org/10.1101/cshperspect.a009316>.
32. Fougère, M., van der Zouwen, C.I., Boutin, J., Neszvecsko, K., Sarret, P., and Ryczko, D. (2021). Optogenetic stimulation of glutamatergic neurons in the cuneiform nucleus controls locomotion in a mouse model of Parkinson's disease. *Proc. Natl. Acad. Sci. USA* 118, e2110934118. <https://doi.org/10.1073/pnas.2110934118>.
33. Zhang, Y., Roy, D.S., Zhu, Y., Chen, Y., Aida, T., Hou, Y., Shen, C., Lea, N.E., Schroeder, M.E., Skaggs, K.M., et al. (2022). Targeting thalamic circuits rescues motor and mood deficits in PD mice. *Nature* 607, 321–329. <https://doi.org/10.1038/s41586-022-04806-x>.
34. Magno, L.A.V., Tenza-Ferrer, H., Collodetti, M., Aguiar, M.F.G., Rodrigues, A.P.C., da Silva, R.S., Silva, J.D.P., Nicolau, N.F., Rosa, D.V.F., Birbrair, A., et al. (2019). Optogenetic Stimulation of the M2 Cortex Reverts Motor Dysfunction in a Mouse Model of Parkinson's Disease. *J. Neurosci.* 39, 3234–3248. <https://doi.org/10.1523/JNEUROSCI.2277-18.2019>.
35. Grossman, R.G. (1958). Effects of stimulation of non-specific thalamic system on locomotor movements in cat. *J. Neurophysiol.* 21, 85–93. <https://doi.org/10.1152/jn.1958.21.1.85>.
36. Wardas, J., Ossowska, K., and Wolfarth, S. (1988). Evidence for the independent role of GABA synapses of the zona incerta-lateral hypothalamic region in haloperidol-induced catalepsy. *Brain Res.* 462, 378–382. [https://doi.org/10.1016/0006-8993\(88\)90569-0](https://doi.org/10.1016/0006-8993(88)90569-0).
37. Périer, C., Tremblay, L., Féger, J., and Hirsch, E.C. (2002). Behavioral consequences of bicuculline injection in the subthalamic nucleus and the zona incerta in rat. *J. Neurosci.* 22, 8711–8719. <https://doi.org/10.1523/JNEUROSCI.22-19-08711.2002>.
38. Power, B.D., and Mitrofanis, J. (1999). Evidence for extensive inter-connections within the zona incerta in rats. *Neurosci. Lett.* 267, 9–12. [https://doi.org/10.1016/s0304-3940\(99\)00313-4](https://doi.org/10.1016/s0304-3940(99)00313-4).
39. Li, L.X., Li, Y.L., Wu, J.T., Song, J.Z., and Li, X.M. (2022). Glutamatergic Neurons in the Caudal Zona Incerta Regulate Parkinsonian Motor Symptoms in Mice. *Neurosci. Bull.* 38, 1–15. <https://doi.org/10.1007/s12264-021-00775-9>.
40. Chometton, S., Barbier, M., and Risold, P.Y. (2021). The zona incerta system: Involvement in attention and movement. *Handb. Clin.*

- Neurol. 180, 173–184. <https://doi.org/10.1016/B978-0-12-820107-7.00011-2>.
41. Gulcebi, M.I., Ketenci, S., Linke, R., Hacıoğlu, H., Yanali, H., Veliskova, J., Moshé, S.L., Onat, F., and Çavdar, S. (2012). Topographical connections of the substantia nigra pars reticulata to higher-order thalamic nuclei in the rat. *Brain Res. Bull.* 87, 312–318. <https://doi.org/10.1016/j.brainresbull.2011.11.005>.
42. Gallay, M.N., Jeanmonod, D., Liu, J., and Morel, A. (2008). Human pallidothalamic and cerebellothalamic tracts: anatomical basis for functional stereotactic neurosurgery. *Brain Struct. Funct.* 212, 443–463. <https://doi.org/10.1007/s00429-007-0170-0>.
43. Aumann, T.D., and Horne, M.K. (1996). Ramification and termination of single axons in the cerebellothalamic pathway of the rat. *J. Comp. Neurol.* 376, 420–430. [https://doi.org/10.1002/\(SICI\)1096-9861\(19961216\)376:3<420::AID-CNE5>3.0.CO;2-4](https://doi.org/10.1002/(SICI)1096-9861(19961216)376:3<420::AID-CNE5>3.0.CO;2-4).
44. Schapira, A.H.V., Chaudhuri, K.R., and Jenner, P. (2017). Non-motor features of Parkinson disease. *Nat. Rev. Neurosci.* 18, 435–450. <https://doi.org/10.1038/nrn.2017.62>.
45. Liu, K., Kim, J., Kim, D.W., Zhang, Y.S., Bao, H., Denaxa, M., Lim, S.A., Kim, E., Liu, C., Wickersham, I.R., et al. (2017). Lhx6-positive GABA-releasing neurons of the zona incerta promote sleep. *Nature* 548, 582–587. <https://doi.org/10.1038/nature23663>.
46. Burrows, A.M., Ravin, P.D., Novak, P., Peters, M.L.B., Dessureau, B., Swearer, J., and Pilitsis, J.G. (2012). Limbic and motor function comparison of deep brain stimulation of the zona incerta and subthalamic nucleus. *Neurosurgery* 70, 125–130. , discussion 130-131; discussion 130-121. <https://doi.org/10.1227/NEU.0b013e318232fdac>.

STAR★METHODS

KEY RESOURCES TABLE

REAGENT or RESOURCE	SOURCE	IDENTIFIER
Antibodies		
rabbit-anti-tyrosine hydroxylase antibody	Millipore	AB152; RRID: AB_390204
Alexa Fluor 488, Donkey anti-Rabbit	Thermo Fisher	A21206; RRID: AB_2535792
mouse-anti-GABA antibody	Sigma	A0310; RRID: AB_476667
Alexa Fluor 555, Donkey anti-Mouse	Thermo Fisher	A31570; RRID: AB_2536180
Alexa Fluor 488, donkey anti-Mouse	Thermo Fisher	A21202; RRID: AB_141607
nNOS Polyclonal Antibody(Mouse Polyclonal)	Thermo Fisher	61-7000; RRID: AB_2313734
Anti-Parvalbumin Antibody(Mouse monoclonal)	Abcam	ab181086; RRID: AB_2924658
Bacterial and virus strains		
pAAV-GAD67-MCS-mCherry-3Flag	OBiO Technology	H2792
pAAV-GAD67-hM3D(Gq)-mCherry-WPRE	OBiO Technology	H15962
pAAV-GAD67-hM4D(Gi)-mCherry-WPRE	OBiO Technology	H15968
pAAV-GAD67-EGFP-3xFLAG-WPRE	OBiO Technology	H3232
pAAV-GAD67-hChr2(H134R)-EGFP-3xFLAG-WPRE	OBiO Technology	H9440
pAAV-GAD67-eNpHR 3.0-EGFP-3xFLAG-WPRE	OBiO Technology	H23266
pAAV-EF1a-DIO-mCherry-WPRE	OBiO Technology	AG20299
pAAV-EF1a-DIO-hChr2(H134R)-mCherry	OBiO Technology	AG20297
Chemicals, peptides, and recombinant proteins		
ClozapineN-oxide dihydrochloride	Tocris	6329; RRID: -
Experimental models: Organisms/strains		
Mouse: C57BL/6JNifdc male mice	Beijing Vital River Laboratory Animal Technology Co., Ltd	C57BL/6J
Mouse: Vgat-Cre male mice	The Jackson Laboratory	Vgat-Cre
Software and algorithms		
Smart v3.0	Panlab/Spain	https://www.rwdls.com/product-solutions/life-sciences/behavior/tracing
CatWalk XT 10.6	Noldus	https://www.noldus.com/catwalk
digital pathological section scanning system	Olympus, Tokyo, Japan, VS120	https://www.olympus-lifescience.com/.../virtual/vs120
GraphPad Prism V.6.0.	Dotmatics	GPS-1123456-ABCD-1234

RESOURCE AVAILABILITY

Lead contact

Further information and requests for resources and reagents should be directed to and will be fulfilled by the lead contact, Limin shi (liminshi@qdu.edu.cn).

Materials availability

All materials used in this study were shown in the [key resources table](#).

Data and code availability

- All data reported in this paper will be shared by the [lead contact](#) upon request.
- This paper does not report original code.
- Any additional information required to reanalyze the data reported in this paper is available from the [lead contact](#) upon request.

EXPERIMENTAL MODEL AND STUDY PARTICIPANT DETAILS

Animals

C57BL/6J and Vgat-Cre male mice aged 6–8 weeks were purchased from Beijing Vital River Laboratory Animal Technology Co., Ltd. A maximum of 4 mice were housed in each cage under constant temperature and humidity on a 12-h light/dark cycle, and adequate food and water were provided. All procedures were performed in accordance with the National Institutes of Health Guide for the Care and Use of Laboratory Animals and were approved by the Animal Ethics Committee of Qingdao University.

Establishment of the 6-OHDA model

A PD animal model was generated using the following detailed procedures.²⁶ First, desipramine hydrochloride (25 mg/kg, Sigma, D3900) was intraperitoneally injected into the mice to protect noradrenergic neurons. After 30 min, the mice were deeply anesthetized with isoflurane and fixed on a stereotaxic frame (RWD, 68018), and isoflurane was given to the mice to maintain anesthesia. Throughout the whole surgery, a heating pad was used to maintain the body temperature of mice and erythromycin ointment was applied to the eyes of mice to prevent the light damage to the eyes. A scalp incision was made with eye scissors. The skull was exposed, and a hole was drilled over the target region with a stereotaxic drill. 6-OHDA (2 $\mu\text{g}/\mu\text{L}$, 2 μL dissolved in 0.2% (w/v) ascorbic acid, Absin, abs44119665) or 0.9% normal saline (NS, as control) was unilaterally or bilaterally injected into the striatum at the appropriate stereotaxic coordinates (AP: 0.4 mm, ML: ± 1.8 mm, DV: -3.5 mm) with a syringe (WPI, Nanoliter 2010) controlled by a syringe pump (WPI, Micro2T) at a rate of 0.6 nl/s. The syringe was left in place for an additional 10 min to allow diffusion of the 6-OHDA, prevent backflow, and then slowly withdraw. After injection, the mice were allowed two weeks for recovery, and the weight of the mice was recorded daily. Two weeks after 6-OHDA injection, the apomorphine (APO, 0.5 mg/kg, Macklin, R828372)-induced rotation test was conducted to evaluate whether the establishment of the 6-OHDA-induced PD mouse model was successful. The rotation number was counted manually 3 min after APO injection, and mice exhibiting more than 40 rotations in 10 min were chosen for the following studies.

Cannula implantation

Two weeks after 6-OHDA injection, mice were deeply anesthetized, and a single guide cannula (RWD Instruments, 62003) was implanted 300 μm above the ZI at the appropriate stereotaxic coordinates (AP: -1.9 mm, ML: 1.4 mm, DV: -4.2 mm) and fixed to the skull with dental cement. After one week of recovery, etomidate (5 $\mu\text{g}/\mu\text{L}$, 1 μL) or bicuculline (5 $\mu\text{g}/\mu\text{L}$, 1 μL) was injected into the ZI at a rate of 0.1 $\mu\text{L}/\text{min}$, and then the mice were subjected to behavioral tests. The cannula placement was checked by immunofluorescence staining after all tests were finished. Only data from animals with correct cannula placement were used.

Virus injection

The mice were deeply anesthetized with isoflurane, and their heads were fixed to a stereotaxic frame (RWD, 68018). A glass syringe containing virus was inserted into the ZI (AP: -1.9 mm, ML: 1.4 mm, DV: -4.2 mm). The virus (100 nL) was injected into the ZI at a rate of 0.3 nL/s, and the syringe was left in place for 10 minutes after the injection to allow virus diffusion. Behavioral tests were performed three weeks after viral expression was successfully induced. After analysis, the mice were perfused, and their brains were collected to confirm that the virus was injected at the correct site. The following viruses were used in this study: pAAV-GAD67-MCS-mCherry-3Flag (titer: 3.86×10^{13} , OBiO Technology), pAAV-GAD67-hM3D(Gq)-mCherry-WPRE (titer: 7.62×10^{12} , OBiO Technology), pAAV-GAD67-hM4D(Gi)-mCherry-WPRE (titer: 3.16×10^{12} , OBiO Technology), pAAV-GAD67-EGFP-3xFLAG-WPRE (titer: 9.39×10^{12} , OBiO Technology), pAAV-GAD67-hChr2(H134R)-EGFP-3xFLAG-WPRE (titer: 8.12×10^{12} , OBiO Technology), pAAV-GAD67-eNpHR 3.0-EGFP-3xFLAG-WPRE (titer: 9.15×10^{12} , OBiO Technology), pAAV-EF1a-DIO-mCherry-WPRE (titer: 2.40×10^{13} , OBiO Technology), and pAAV-EF1a-DIO-hChr2(H134R)-mCherry (titer: 7.08×10^{12} , OBiO Technology).

METHOD DETAILS

Optogenetic manipulation

Three weeks after induction of virus expression, an optical fiber (Inper Ltd, Hangzhou, China) with a diameter of 200 μm was implanted 200 μm above the virus injection site in the ZI. The ceramic ferrule at the top of the fiber was fastened to the skull with two screws and dental cement. After recovery for at least a week, behavioral tests were performed. The mice were acclimated to handling for three consecutive days before the test to minimize stress. Then, light with a wavelength of 473 nm (blue light) or 593.5 nm (yellow light) was delivered to mice expressing ChR2, NpHR, and EGFP by a fiber-connected laser (QAXK-LASER, Thinker Tech Nanjing Bioscience Inc). The intensity of the laser light was calculated using an optical power meter (QAXK-CCP) at the end of the fiber. The intensity was controlled at 5 mW (473 nm, 30 Hz, 5 ms pulse width) for blue light and 10 mW (593.5 nm, continuous light stimulation) for yellow light. For bilateral light stimulation, the output was adjusted so that the same amount of light was delivered to both sides.

Chemogenetic manipulation

For chemogenetic manipulation, before each behavioral test, the mice were intraperitoneally injected with CNO (Tocris, 6329) or NS. For pharmacological manipulation, etomidate, bicuculline or NS was microinjected into the ZI. The behavioral test was performed within half an hour after injection.

Rotation test

The APO-induced rotation test is a widely used method to judge the success of unilateral 6-OHDA injection in establishing a PD model. Two weeks after 6-OHDA injection, the mice were intraperitoneally injected with APO (0.5 mg/kg, Macklin, R828372), placed in a transparent resin cylinder with a diameter of 30 cm and monitored by video from above. After five minutes, the number of turns was recorded manually. If the number of rotations within ten minutes exceeded forty, the PD model was considered successfully established. Subsequent tests were carried out with mice in which PD was successfully induced.

Open-field test

The open-field test was used to assess motor behavior and anxiety in mice. The mice were placed in the center of a 27 \times 27 \times 35 cm open box, and a camera was placed directly above the box. The Smart v3.0 system was used to record the behavior of the mice for 10 minutes. The optogenetic experiments performed the test in three consecutive three-minute phases: pre, light, and post. The open-field arena was cleaned with 75% alcohol and allowed to dry between trials. In the open-field test, we analyzed the total distance traveled, average movement velocity, and central zone exploration time (%) of mice.

Rotarod test

The rotarod test can be used to detect changes in motor coordination of mice. Using a programmable acceleration device (Med Associates, USA), mice were first acclimated on a stationary rotarod for 2 minutes facing a wall. The device rotation speed was set to 4~40r/min, and the cutoff time was 5 minutes. After the experiment started, the system automatically recorded the length of time and the rotation speed of the device that the mouse stayed or fell off the rotarod. Two times recording was obtained by discontinuous measurement, and the time interval is more than 1 hour between the two measures. The longer the mice stayed on the rotarod device, the faster the rotational speed when it fell off, indicating better motor coordination and vice versa.

Pole test

The pole test was used to evaluate the motor coordination of mice. The custom pole climbing apparatus consisted of an approximately 50 cm long (1 cm in diameter) pole placed perpendicular to the ground. The day before the test, each mouse was trained to climb from the top to the bottom of the pole by placing it on the top of the pole facing upward. The time it took each mouse to climb from the top to the bottom of the pole was recorded on the test day. Two measurements were obtained half an hour apart, and the mean data was calculated.

Balance beam test

The balance beam test was used to detect changes in the balance of mice. The apparatus consisted of a 1 meter (1.2 cm in diameter) round wooden stick elevated 50 cm above the ground. The day before the test,

the mice were trained to walk on the balance beam. In the test phase, the mice were placed at the end of the balance beam. The mice were observed as they crossed the balance beam, and the balance of the mice was evaluated according to the modified rating scale described by Feeney et al.²⁷ Repeated measurements were taken at half-hour intervals, and mean data was calculated.

Gait analysis

Gait analysis was performed to evaluate the motor coordination and postural stability of mice via measurement of a variety of static and dynamic indicators (such as base of support, swing phase, support mode, and normal step ratio). The CatWalk XT (Noldus) automatic gait analysis system and a high-speed camera placed under a glass runner were used to capture the footprints of the mice using footprint light refraction technology. The mice were trained a day in advance to run continuously from one end of the glass track to the other. On the test day, the mice were acclimated to the test environment for at least half an hour. The mice were placed in the apparatus and allowed to run down the track, ensuring that at least 3 valid runs were collected for each mouse. CatWalk XT 10.6 software was used to analyze the appropriate parameters.

Immunofluorescence staining

After all behavioral tests, the mice were deeply anesthetized and transcardially perfused with 0.9% NaCl and 4% paraformaldehyde (PFA). The brains were carefully removed and placed at 4°C in 4% PFA for at least 6 h. Gradient dehydration was then performed with 20% and 30% sucrose (dissolved in 0.1 M PBS) until the brains sank. The tissues were cut into 20 µm thick coronal sections with a freezing microtome (Leica, CM1900) and collected for subsequent immunofluorescence staining. The sections were incubated with PBST (0.3% Triton-100 in PBS) blocking buffer containing 5% donkey serum (Jackson, 017-000-001) for one hour at room temperature. The sections were then incubated overnight with relevant primary antibodies (rabbit-anti-tyrosine hydroxylase antibody: Millipore, AB152, 1:1000; mouse-anti-GABA antibody: Sigma, A0310, 1:300; nNOS Polyclonal Antibody: Thermo Fisher, 61-7000, 1:300; Anti-Parvalbumin Antibody: Abcam, ab181086, 1:100) at 4°C. The sections were incubated with fluorescent secondary antibody (Alexa Fluor 488, Donkey anti-Rabbit: Thermo Fisher, A21206, 1:500; Alexa Fluor 555, Donkey anti-Mouse: Thermo Fisher, A31570, 1:500; Alexa Fluor 488, donkey anti-Mouse: Thermo Fisher, A21202, 1:500) at room temperature for 2 hours. Following previously described methods,^{28,29} the number of GABAergic neurons in the ZI was counted bilaterally from at least six sections per animal. Counts were made from comparable sections across the full rostro-caudal extent of the ZI (rZI: two sections, dZI/vZI: two sections, rZI: two sections). A digital pathological section scanning system (Olympus, Tokyo, Japan, VS120) was used for imaging.

High-performance liquid chromatography (HPLC) with electrochemical detection

The striatum was carefully isolated and transferred to liquid nitrogen for storage until analysis. Then, the samples were weighed and homogenized in 0.3 ml of liquid A (0.4 M perchloric acid). After the first centrifugation at 12000 rpm for 20 min at 4°C, supernatant (80 µl) was transferred to an Eppendorf tube and mixed with 40 µl of liquid B (20 mM citramalic acid potassium, 300 mM dipotassium phosphate, 2 mM EDTA·2Na). The samples were centrifuged again at 12000 rpm for 20 min at 4°C. Then, the levels of DA and its metabolites DOPAC and HVA in 100 µl of the supernatant were measured by HPLC.³⁰ The separation was performed on a PE C₁₈ reversed-phase column with a mobile phase consisting of 20 mM citramalic acid, 50 mM sodium caproate, 0.134 mM EDTA·2Na, 3.75 mM sodium octane sulphonic acid, and 1 mM di-sec-butylamine with a flow rate of 1 ml/min and containing 5% (v/v) methanol. A 2465 electrochemical detector (Waters, USA) was used to detect the compounds in screen mode. The results were reported as ng/mg wet weight of brain tissue.

QUANTIFICATION AND STATISTICAL ANALYSIS

Statistical analysis

All data are presented as the mean ± SEM. GraphPad Prism V.6.0. was used for data analysis. Column statistics was first used to test the data for normal distribution. Unpaired t tests were used for comparisons between two groups, and two-way analysis of variance (ANOVA) and Sidak's multiple comparison tests were used for comparisons among multiple groups. The optogenetic experiments were analyzed by two-way ANOVA with Bonferroni post hoc analysis. The nonparametric or not-normally distributed data were analyzed by Mann-Whitney U and Kruskal-Wallis tests with Dunn's post hoc tests to compare two groups or multiple groups, respectively.